Computer Networks 112 (2017) 108–121

Contents lists available at ScienceDirect

Computer Networks

journal homepage: www.elsevier.com/locate/comnet

A partial feedback reporting scheme for LTE mobile video transmission with QoS provisioning

Mustafa Ismael Salman[a,b,*], Muntadher Qasim Abdulhasan[a], Chee Kyun Ng[a], Nor Kamariah Noordin[a], Borhanuddin Mohd Ali[a], Aduwati Sali[a]

[a] Department of Computer and Communication Systems Engineering, Faculty of Engineering, University Putra Malaysia, UPM Serdang, 43400 Selangor, Malaysia
[b] Department of Computer, Faculty of Engineering, University of Baghdad, Baghdad, Iraq

ARTICLE INFO

Article history:
Received 4 June 2015
Revised 27 August 2016
Accepted 6 September 2016
Available online 16 September 2016

Keywords:
Channel quality indicator (CQI)
Long term evolution (LTE)
Partial feedback
Quality-of-service (QoS)

ABSTRACT

Opportunistic frequency-domain scheduling and link adaptation enable the long term evolution (LTE) cellular systems to maximize the throughput. Successful scheduling and link adaptation require perfect channel state information (CSI) at the eNodeB. However, for multi-carriers systems, a huge undesirable amount of signaling overhead is required to report the channel quality indicator (CQI) for the whole bandwidth. On the contrary, reducing the size of CQI overhead detriments the downlink performances and does not guarantee the quality-of-service (QoS) when real-time multimedia services are applied. As a consequence, a tradeoff between CQI overhead and the downlink performances is presented in this paper. Then, an Adaptive Threshold CQI Partial Feedback (ATCPF) scheme is proposed by using multi-objective swarm intelligence to find the optimal feedback threshold. Based on an LTE system-level simulation, significant enhancements of 20% and 38% in throughput and packet loss ratio (PLR) respectively are obtained compared to a fixed threshold feedback. Since video flows are considered, a self-optimized partial feedback (SOPF) is further developed by using cross-layer optimization to guarantee QoS. The results show that the feedback overhead is minimized at low-load network condition while maintaining the PLR below its target. The proposed algorithm provides a high flexibility in responding to certain variations, and it enables the cellular systems to support multimedia services.

1. Introduction

Multiuser diversity is exploited to enhance system throughput in wireless multiple-access communications. Such diversity is obtained by using an opportunistic user scheduling for a frequency selective shared channel [1]. Intelligent resource allocation with orthogonal frequency division multiple access (OFDMA) systems can also be employed to further exploit the multiuser diversity [2,3]. For downlink transmission of long term evolution (LTE) cellular systems, OFDMA has been selected as a multiple access scheme due to its efficiency and low complexity [4]. In the frequency domain, the whole bandwidth is divided into several resource blocks (RBs), each consists of twelve 15 kHz subcarriers. Each RB can be exclusively allocated to one user at a time. The allocation process depends on the channel status of different users on that RB. In order to maximize LTE downlink performances, the eNodeB should have perfect channel state information (CSI) for all users with respect to the available RBs. Therefore, each user has to report its channel quality via a 4-bit uplink word, which is called a channel quality indicator (CQI) [5,6]. The fullband CQI feedback scheme, where each user reports the signal-to-interference-plus-noise ratio (SINR) on each RB to eNodeB, is proposed [7]. Although CQI feedback requires only few bits per RB, it is still impractical in modern LTE cellular communications to let all users report the CQI for all RBs. Specifically, the fullband CQI feedback scheme is not spectrum- and energy-efficient due to the high signaling overhead produced.

Therefore, several CQI reduction schemes are introduced. The most well investigated scheme is a wideband CQI reporting scheme [4]. By using this method, the mobile terminal has to generate one averaged feedback to represent the quality of whole channel bandwidth. Although this scheme produces the lowest signaling overhead, the obtained averaged CQI does not reflect the real channel status for all RBs and, thus the opportunistic frequency domain scheduling is no longer possible. Other optimized feedback method is the best-M CQI [8,9]. In this scheme, the user equipment (UE) reports back the RBs that have the highest CQI values, as well as

* Corresponding author.
E-mail address: mustafa.i.s@ieee.org (M.I. Salman).

http://dx.doi.org/10.1016/j.comnet.2016.09.004
1389-1286/

the location indices of these best-M RBs, where "M" is a design parameter to specify the number of RBs with the highest CQI. Although low value of "M" reduces the feedback signaling overhead, it degrades system throughput [10]. Further reduction in feedback information size can be obtained by using a threshold based CQI reporting scheme [11,12]. In this scheme, a UE will be able to report three values; the first and second values represent the average CQIs of the RBs with SINR higher and lower than a certain threshold relative to the highest measured CQI. The third one is a bit mask which indicates the location of the RBs included within the first averaged value. The best threshold value is between 4 and 5 dB as shown in [13]. A hybrid of best-M and threshold based feedback schemes was developed by the authors in [14]. However, it was observed that the hybrid scheme has the signaling overhead as the pure threshold based CQI feedback [15]. For LTE systems, a subband-level CQI feedback scheme is specified [16,17]. In this scheme, the channel bandwidth is divided into Z subbands such that the UE feeds back one CQI word per each subband. The number of subbands (Z) is a design parameter to optimize the overall system performances. More considerable work on the joint analysis between frequency domain scheduling and feedback schemes has also been achieved in [14,18,19]. The authors have analyzed the throughput obtained by both best-M and threshold based feedback schemes with different packet schedulers. The throughput of proportional fair (PF) with fullband and partial feedback was studied and analyzed in [20]. In addition to CQI, the precoding matrix indicator (PMI) and rank indicator are also required to be reported by a UE to eNodeB when MIMO antenna systems are considered [21–23], however, they are out of the scope of this paper.

While CQI feedback overhead reduction is crucial, especially in a multiple-access frequency selective channel, the CQI value produced by the aforementioned feedback schemes does not represent the actual SINR of all RBs and, thus, the system performance will be degraded in two folds [18]. First, degradation can be obtained when the reported CQI is less than the actual CQI. In this case, the eNodeB transmits at a lower rate corresponding to the reported averaged CQI and, therefore, system throughput will be decreased. The second degradation is produced when the reported CQI is larger than the actual SINR of the n-th RB. This case will let the eNodeB to transmit with a modulation and coding scheme (MCS) larger than the threshold which leads to a failed decoding process. Failure in decoding the resource elements on that RB will cause an outage, and the resulted throughput will be 0 on that RB. Although most of the state-of-the-art CQI feedback schemes trying to reduce the impact of feedback reduction on downlink performance, more enhancements are required to optimize CQI overhead with minimum outage and throughput loss, which is the scope of this paper.

In this paper, different CQI feedback schemes are presented and compared. Then, an Adaptive Threshold-based CQI Partial Feedback (ATCPF) scheme is adopted by using a multi-objective particle swarm optimization (PSO). The ATCPF aims to find the optimal SINR threshold value at every CQI reporting interval, which is a multiple of transmission time interval (TTI). The optimal threshold value will achieve minimum CQI overhead and outage capacity while maximizing the system throughput in downlink transmission. Since the overhead can be minimized at the cost of throughput and outage capacity, simple additive weight (SAW) algorithm is used to find the best threshold alternative produced by these conflicting criteria. It seems that the method of SAW is a multi-criteria decision making methods that used for weight determinations and preferences. In addition to its simplicity in implementaton, the advantage of SAW method is that it is a proportional linear transformation of the raw data. It means that the relative order of magnitude of the standardized scores remains equal [27]. Among other heuristic methods, PSO is also used to determine the optimal SINR threshold value that achieves the best tradeoff between uplink signaling overhead and downlink performances. PSO is used in the proposed algorithm because it has less control parameters to be tuned by the user, and thus, its computational burden is relatively low. Furthermore, it provides fast convergence [28].

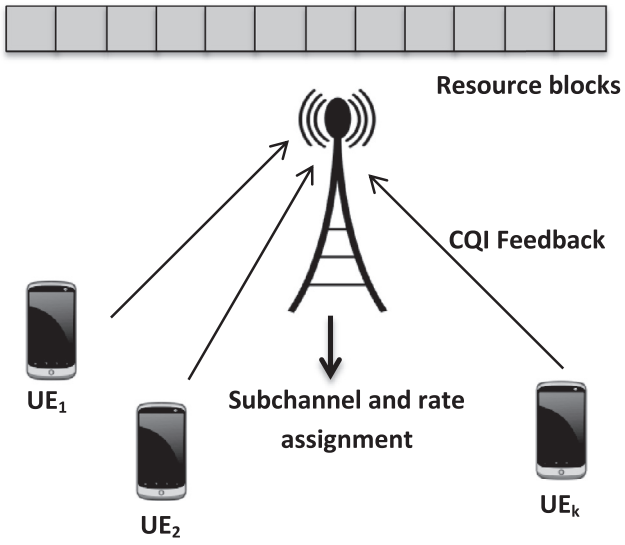

Fig. 1. System model.

By using a hybrid of PSO and SAW, the impact of overhead reduction can be adapted according to many parameters, e.g. network load condition. Furthermore, the impact of the ATCPF algorithm on the quality of service (QoS) is highlighted. Then, a Self-Optimized Partial Feedback (SOPF) algorithm is developed by using cross-layer optimization. In this algorithm, the amount of feedback overhead is controlled such that the QoS parameters will not be forfeited.

The rest of the paper is structured as follows. In Section 2, the system model and problem formulation are discussed. In Section 3, the proposed adaptive threshold based CQI feedback scheme is demonstrated. The self-optimized partial feedback is explained in Section 4. Section 5 is then emphasizes the computational complexity of the proposed algorithm. Then, the performance evaluation and discussion is conducted in Section 6. Finally, the conclusion will be drawn in Section 7.

2. System model and problem formulation

2.1. System model

In this paper, an eNodeB serving K users is considered as shown in Fig. 1. The physical resources are multiplexed between users in time and frequency domain. The allocation of RBs depends on the channel experienced by each user. The channel behavior across those RBs are assumed to be independent and identically distributed [18,24]. In order to achieve opportunistic scheduling and resource allocation, each user should report a CQI back to the eNodeB. As shown in Fig. 2, the CQI generation process starts by estimating the SINR for all allocated subcarriers at the receiving terminal by using an appropriate channel estimation technique. Considering that the subcarriers belonging to nth RB are transmitted over a flat fading channel. Then, the $SINR_n$ will be mapped into discrete values which represent the index of CQI by quantization steps as

$$CQI_{dB}(n) = QStep_{dB} * floor\left(\frac{SINR_{dB}(n)}{QStep_{dB}} + 0.5\right) \quad (1)$$

The CQI quantized values are reported to the eNodeB either periodically or aperiodically. The periodicity and frequency resolution

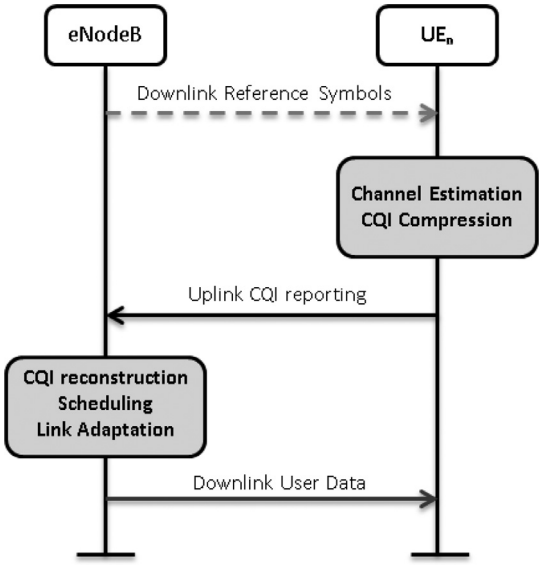

Fig. 2. CQI reporting procedure.

to be used by a UE to report the CQI values are controlled by the eNodeB. The periodic CQI reporting is attained through the Physical Uplink Control Channel (PUCCH), while the aperiodic reporting is attained through the Physical Uplink Shared Channel (PUSCH) by using a specific reporting scheme. The CQI reporting delay is assumed to be negligible [18]. According to the reported CQI quantized values, packet scheduling and resource allocation will be performed at the eNodeB.

Since video flows are considered, the Modified Largest Weighted Delay First (M-LDWF) scheduler is used to guarantee packet delivery within a certain deadline to avoid packet drops. The related scheduling metric is expressed as

$$m_{n,k} = -\frac{\log \zeta_k}{\tau_k} D_{HOL_k} \cdot \frac{r_{n,k}}{\bar{R}_k} \tag{2}$$

where ζ_k is the maximum probability that the delay of the head of line (D_{HOL_k}) packet exceeds its delay threshold (τ_k), $r_{n,k}$ is the instantaneous rate that has been achieved by user k hosting the n-th flow, and $\bar{R}_k$ is the average data rate.

2.2. Problem formulation

The CQI generation process starts by estimating the SINR for all allocated subcarriers at the receiving terminal by using an appropriate channel estimation technique. Considering that the subcarriers belonging to nth RB are transmitted over a flat fading channel. Then, the SINR$_n$ will be mapped into discrete values which represent the index of CQI by quantization steps as

$$CQI_{dB}(n) = QStep_{dB} * floor\left(\frac{SINR_{dB}(n)}{QStep_{dB}} + 0.5\right) \tag{3}$$

The feedback overhead becomes a more serious problem in multichannel systems like OFDMA systems that have tens of shared channels. If every active user sends feedback data for all channels, it consumes a lot of uplink bandwidth [14]. For example, an emerging system in Korea, the IEEE 802.16e-based WiBro system is expected to encounter this problem in the AMC mode.2 If each user sends the feedback on the states of its 24 channels, the total amount of CQI becomes very large [14].

The basic feedback scheme introduced by the third generation partnership project (3GPP) for LTE systems is the fullband CQI scheme. In this scheme, the CQI per each RB is reported to the eNodeB.Therefore, the feedback signaling overhead (ϕ) produced by

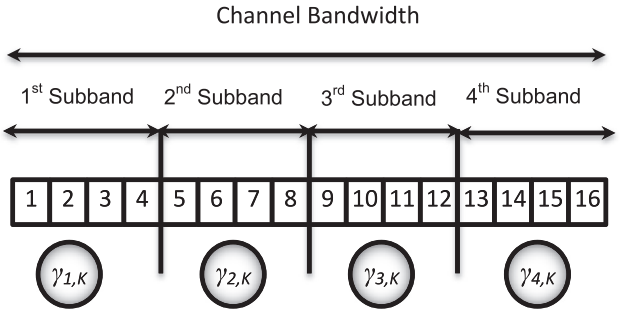

Fig. 3. Subband-level CQI reporting scheme.

using this scheme is calculated as

$$\phi = N_{RB} \times S \tag{4}$$

where N_{RB} is the number of RBs, and S is the number of bits required to represent the CQI indexed value, i.e. 4-bits are required to represent CQI for LTE cellular networks. Such signaling overhead is relatively high, especially when all users have to report their channel quality periodically at every CQI reporting interval. To reduce the size of CQI overhead, many schemes have been investigated in the literature as explained below.

2.2.1. Subband-level [16,17]

Instead of reporting one CQI per each RB as in the full band reporting scheme, a CQI word is reported per each channel subband which represents more than two contiguous RBs as shown in Fig. 3. The reported CQI represents the effective SINR of user k for the subband z ($\gamma_{z,k}^{eff}$) which is calculated by using the effective exponential SNR mapping (EESM) as [25] (Appendix A)

$$\gamma_{z,k}^{eff} = -\lambda \ln\left(\frac{1}{Z}\sum_{n\in RBs} e^{-\frac{\gamma_{n,k}}{\lambda}}\right) \tag{5}$$

where λ is a parameter that is empirically calibrated for each MCS. The size of signaling overhead required to report CQI for Z subbands is

$$\phi_{sub} = S \times Z \tag{6}$$

2.2.2. Threshold-based feedback scheme [11]

Further overhead reduction can be achieved when threshold-based feedback scheme is used. The users report the CQI values for RBs which are included within a threshold relative to the highest measured CQI together with the corresponding positions. First, the best RB within the full bandwidth is identified with its corresponding CQI. The highest CQI value represents the upper bound of the considered threshold window, which embeds the RBs with the best CQI values. The size of the threshold window is a design parameter to be decided by higher layers. Then, the CQIs of the best RBs are reported as a single averaged CQI value (S bits), together with a bit-mask for the whole RBs (N_{RB}) which indicates the position of the reported RBs. Moreover, the remaining RBs are also reported as a single averaged CQI value (S bits). Therefore, the signaling overhead required when using threshold-based reporting scheme is

$$\phi_{thr} = 2S + N_{RB} \quad (bits) \tag{7}$$

Although the feedback reduction scheme is crucial for uplink transmission, it causes a performance degradation throughout the downlink transmission. Specifically, the throughput will be reduced due to wrong scheduling decision (outage), and lower rate transmission [18]. Therefore, a tradeoff between CQI overhead, throughput and the outage capacity will be emphasized in this paper. Fur-

thermore, the impact of the proposed algorithm on the QoS will also be highlighted.

3. Adaptive threshold CQI partial feedback (ATCPF)

Two averaged values, as those reported by a fixed threshold scheme, may not be sufficient to express the status of the whole channel bandwidth, especially when the channel suffers from deep selective fading. Accordingly, we proposed that the RBs with SINR higher than the specified threshold to be reported individually due to their significance compared to RBs with low SINR. However, huge signaling overhead can be obtained when most of reported RBs are within the threshold window. On the contrary, one averaged word for the low-quality RBs may not be sufficient to express the quality of the channel when most of the RBs have CQI less than the threshold. Therefore, finding the optimal threshold at each CQI reporting interval is crucial to maximize the downlink throughput and minimize the outage capacity. The ATCPF scheme searches for the optimal threshold such that it can be adapted according to the reported channel conditions to maximize the downlink throughput while keeping the outage and feedback overhead as low as possible. This method will fnd the best balancing between uplink overhead and the downlink performances. Moreover, it the first work that considers the outage capacity of the RBs with CQIs less than the threshold value.

At each CQI reporting interval, a PSO algorithm is used to find the optimal threshold at which the overall system performances will be optimized. The PSO is a population based computational method that was developed by Kennedy and Eberhart [26]. It is inspired by a social behavior of swarms such as ants marching or bird flocking. PSO maintains swarm of particles, each represents a candidate solution to the optimization problem. These particles are flown with specified velocity and direction through a search-space. The particles' positions are iteratively accelerated towards an optimum solution according to their own best positions (personal best) and that encountered by their neighbors (global best). The performance of each particle is evaluated according to a predefined fitness function which is related to the given problem. To find the optimal threshold for the proposed CQI reporting scheme, the following parameters will be identified.

3.1. Fitness function

It represents the objective function of the problem being solved. For the proposed CQI reporting scheme, the fitness function consists of three conflicting criteria, namely, throughput, CQI overhead and the outage capacity. The throughput achieved by the downlink transmission needs to be maximized. However, throughput maximization can be achieved when the most accurate CSI is available at the eNodeB and, thus, more signaling overhead is required. Reducing the CQI signaling overhead will increase the probability of transmitting the corresponding RBs with MCS higher than its threshold and, consequently, the wrongly decoded RBs will be increased. Therefore, the downlink throughput considered as a benefit criterion, while CQI overhead and outage capacity are considered as cost criteria. Simple Additive Weighting (SAW) [27] method is used to formalize the fitness function. By using SAW method, the multi-objective fitness function can be changed into a single objective function by simply adding the competing criteria resulted from each alternative. Moreover, the considered performance criteria can be prioritized by setting a priority weight associated with each criterion according to cellular operator preferences. Mathematically, the fitness function can be formulated as

$$\max_i \sum_{b=1}^{B} w_b f_b(i) = w_1 R(i) + w_2 \varphi(i) + w_3 \phi(i) \tag{8}$$

where $f(i)$ represents the performance of the competitive criteria resulted by i-th particle in the search space, and w is the weighting parameter which is usually normalized as

$$\sum_{b=1}^{B} w_b = 1. \tag{9}$$

Since the three criteria are different and conflict to each other, the normalized criteria will be considered to make them dimensionless and comparable according to whether they are benefit or cost criteria, i.e. the throughput is normalized as in (10), while the overhead and outage capacity are normalized as in (11)

$$R_n(i) = \frac{R(i)}{R_{\max}} \tag{10}$$

$$\phi_n(i) = \frac{\phi_{\max}}{\phi(i)} \tag{11}$$

Therefore, the fitness function is

$$\max_i \sum_{b=1}^{B} w_b f_b(i) = w_1 R_n(i) + w_2 \varphi_n(i) + w_3 \phi_n(i) \tag{12}$$

3.2. Search space (swarm)

It is the space that embeds all the feasible solutions. Mainly, the search space is upper-bounded by the best experienced SINR, and lower-bounded by the worst experienced SINR. Then, the search space for the optimal threshold value will be between these two values, i.e.

$$D(i) = (\gamma_{\max}, \gamma_{\min}) \tag{13}$$

3.3. Swarm size

The swarm size, or population size (P), represents the number of feasible threshold values (particles) inside the search space. After determining the search space, a number of threshold values within the search space are randomly generated. A large swarm size may reduce the number of iterations required to get the optimal threshold value. However, it will increase the computational complexity per iteration. In our algorithm, the candidates for SINR threshold values are chosen to be uniformly distributed within the swarm, and they are listed as below

$$\begin{aligned} &\left(\gamma_{\max} - \frac{D(i)}{P}\right), \\ &2 \times \left(\gamma_{\max} - \frac{D(i)}{P}\right), \\ &\vdots \\ &P\left(\gamma_{\max} - \frac{D(i)}{P}\right) \end{aligned} \tag{14}$$

3.4. Neighborhood topology

It determines the method of interaction between the particles in the swarm and influences their movements. In this paper, a star social topology, where each particle can be influenced by social information obtained from all the particles in the entire swarm, is considered. This method is called a global best PSO, or G_{best} PSO, which is summarized by a flowchart as shown in Fig. 4. In our proposed algorithm, each SINR threshold candidate value in the swarm γ_i has a current position x_i, a current velocity v_i, and a

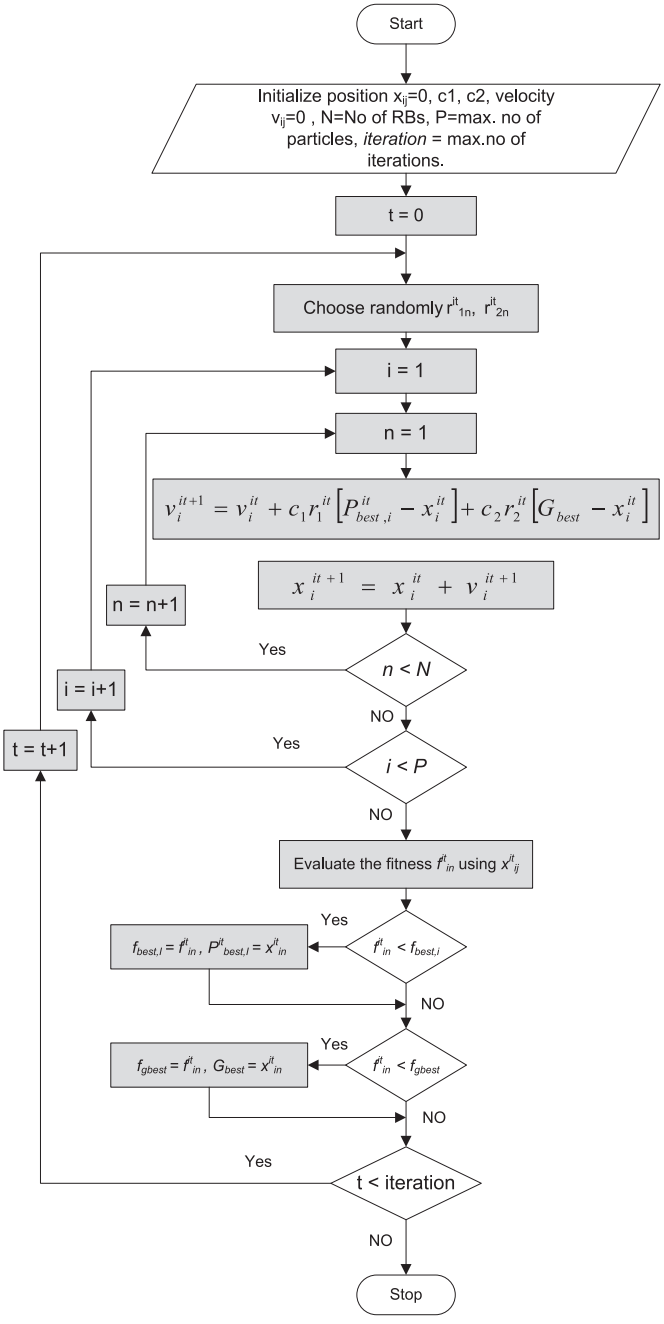

Fig. 4. Flowchart of global best PSO.

personal best position in the search space $P_{best,i}$, which represents the maximum weighted sum achieved by the objective function for the particle *i*. The largest value amongst all the personal best $P_{best,i}$ is called the global best G_{best} which represents the best threshold value obtained by the current iteration. In order to find the optimal threshold value that maximizes the fitness function, $P_{best,i}$ and G_{best} are updated respectively at each iteration as follows

$$P^t_{best,i} = \begin{cases} P^t_{best,i} & \text{if} \quad f(x_i^{t+1}) < P^t_{best,i} \\ x_i^{t+1} & \text{if} \quad f(x_i^{t+1}) \geq P^t_{best,i} \end{cases} \tag{15}$$

$$G_{best} = \max\left\{P^t_{best,i}\right\}$$

After updating the P_{best} and G_{best} for particle *i* at iteration *t*, the CQI threshold value will update its current position x_i^t to a new one x_i^{t+1} as follows

$$x_i^{t+1} = x_i^t + v_i^{t+1} \tag{16}$$

where v_i^{t+1} is the velocity that drives particle *i* toward best and global positions as

$$v_i^{t+1} = v_i^t + c_1 r_1^t\left[P^t_{best,i} - x_i^t\right] + c_2 r_2^t\left[G_{best} - x_i^t\right] \tag{17}$$

As in (17), the update of the particle's velocity can be controlled by three components

1. The inertia component, which is characterized by v_i^t. This component provides the last movement direction for each SINR threshold value γ_i to prevent it from drastically changing direction.
2. The cognitive component, which is denoted by $c_1 r_1^t[P^t_{best,i} - x_i^t]$. This component will measure the performance of each threshold candidates relative to previous performance. In this case, the particles can retrieve their best position that satisfies them during the past iterations.
3. The social component which is characterized by $c_2 r_2^t[G_{best} - x_i^t]$. With the aid of this term, the algorithm can measure the performance obtained by each threshold value with respect to the performances obtained by its neighbors. In this case, the velocity and position of this particle γ_i can move towards the best position obtained by the particle's neighbors.

The cognitive and social components can be differentiated by the weighting parameters c_1 and c_2, which control the relative importance of particle's private experience versus swarm's social experience. Normally, the values of c_1 and c_2 can be found empirically to optimize the search ability of the algorithm by moving the new position of γ_i either towards its own previous best position or the globally best position [28]. In particular, better global exploration inside the swarm space can be obtained when c_1 and c_2 are chosen to be higher values, but it may cause algorithm divergence. On the other hand, refined local search around the best position can be obtained when c_1 and c_2 are small values; however, a large number of iterations are required to find the optimal SINR threshold value.

Different empirical studies suggest that the two accelerating components should be $c_1 = c_2 = 2$, which gives reasonable results for certain applications [28]. Nevertheless, an enhanced approach for optimizing particles' movement in the search space was proposed by Shi and Eberhart [29] as described by (18). In this approach, which is already considered in this paper, a linearly decreasing inertia weighting parameter is multiplied by the velocity term to control the movement of the particle. By initializing the weighting parameter with a high value (from 0.9 to 1.2), the particles will quickly explore the global optimal space. Then, the inertia weight will gradually decrease to a small value (from 0.1 to 0.4) to refine the search process around the optimal region. Therefore, the velocity equation shown by (17) is rewritten as follows

$$v_i^{t+1} = w_v v_i^t + c_1 r_1^t\left[P^t_{best,i} - x_i^t\right] + c_2 r_2^t\left[G_{best} - x_i^t\right] \tag{18}$$

where w_v represents the inertia weighting parameter.

4. Self-optimised partial feedback (SOPF)

The improved cellular networks were designed to meet the continuously increasing demands for wireless data traffic. This means that the LTE QoS, which is based on the evolved packet system (EPS) bearer model, must be top notch. An EPS bearer is a virtual traffic channel to be created between a UE and a gateway for every differentiated traffic flow. Based on its QoS requirement, an EPS bearer can be classified as either a default or a dedicated bearer. The default bearer is assigned once a UE is connected to an LTE

Table 1
LTE QoS parameters.

QCI	Type	PDB[ms]	Packet error rate (PER)	Example service
1	GBR	100	10^{-2}	Conversational voice
2	GBR	150	10^{-3}	Conversational video
3	GBR	300	10^{-6}	Non-conversational video (buffered streaming)
4	GBR	50	10^{-3}	Real time gaming
5	Non-GBR	100	10^{-6}	IMS signaling
6	Non-GBR	100	10^{-3}	Voice, video, interactive gaming
7	Non-GBR	300	10^{-6}	Video (buffered streaming)

network. This bearer can offer only a best-effort service between a UE and a gateway. When a guaranteed bit rate (GBR) service is applied, e.g. real-time voice or video application, a dedicated EPS bearer is assigned in order to give an appropriate treatment to specific services. A set of QoS parameters is associated to each bearer to be distinguished from other bearers, such as bit rate, packet delay budget, packet loss ratio, and scheduling policy. According to these parameters, each type of traffic flows will be prioritized over the others by assigning a specific QoS class identifier (QCI) as shown in Table 1.

In the radio link control layer, the internet protocol packets will be processed and delivered to the packet data convergence protocol (PDCP) layer. However, some of the packets will not be delivered successfully and will be dropped because of several reasons:

- Expiration of the delay deadline (τ_i) of the head-of-line (HOL) packet in the medium access control queue;
- The filled MAC buffer, which blocks the arrived packets until a few of the packets are processed and free space for the new packets is obtained; and/or
- The physical errors caused by transmission channel.

However, the best case configuration should feature a high flexible QoS framework to withstand current limitations and future challenges. One of the current limitations of the partial CQI feedback scheme proposed in the previous section is that it will not guarantee the QoS when GBR traffic is used. It is shown that SINRs averaging for the entire bandwidth RBs will increase the number of RBs that are decoded incorrectly and, thus, the PLR will be increased. In order to guarantee QoS requirement per each bearer and maintain user satisfaction, the PLR should be kept below its target (PLR_{tar}). Therefore, the SOPF algorithm is developed such that the weight parameter per each objective is tuned following the current network condition to guarantee QoS.

The SOPF algorithm starts by initializing the swarm to be consisting of a uniform distribution of SINR threshold values. The PSO

Table 2
Pseudocode of SOPF algorithm.

SOPF algorithm

Initialization: c_1, c_2, w_v, Δw_v, *iteration*
The swarm is initialized with uniform distribution of γ_{thr} between γ_{max} and γ_{max}
while *time* ≤ *Simulation time* **do**
  for *it*:= 1: specified number of *iteration* **do**
    for *i*:= 1: Swarm-size (*P*) **do**
      for *n*:= 1: RB-size (*N*) **do**
        If $\gamma_{i,n} > \gamma_{max}$-$\gamma_{thr}$ **then**
          Update the *overhead*,
          $\phi(x) \leftarrow (\phi(x)+1)\times S + S$
        else
          find γ_{avg} of RBs with $\gamma_{i,n} < \gamma_{max}$-$\gamma_{thr}$
        if $\gamma_{avg} > \gamma_{i,n}$ **then**
          Update the number of RBs in *outage*,
          $\varphi(n) \leftarrow \varphi(n)+1$
        end if
        Map $\gamma_{i,n}$ to corresponding MCS (Table 7.2.3-1 in [4])
        Map MCS to corresponding Block size according to Transport Block size [4]
        $R_{i,n}$ =*TBS(mcs)*
        Update the *throughput*, $R(n) = R(n) + R_{i,n}$
    end for
    Calculate the weighted *fitness*, *f(x,w)* as (12)
    P_{best} is updated according to (15)
    G_{best} is updated according to (15)
    Position and *velocity* are evaluated as new population based on (18)
    fitness is computed for new population
  end for
  $w_v = w_v - (\Delta w_v \,/\, iteration)$
end for
if $SINR_{avg} \langle SINR_{eff}$ **or if** $D_{HOL} \rangle \tau_i$ **then**
  Update dropped Packets, $P_d \leftarrow P_d + 1$;
end
Calculate PLR
if $PLR > PLR_{tar}$ **then**
  $w_1 \leftarrow w_1 + \Delta w$;
  $w_2 \leftarrow w_2 + \Delta w$;
  $w_3 \leftarrow w_3 - \Delta w$;
else
  $w_1 \leftarrow w_1 - \Delta w$;
  $w_2 \leftarrow w_2 - \Delta w$;
  $w_3 \leftarrow w_3 + \Delta w$;
end
Update w_1, w_2 *and* w_3
end

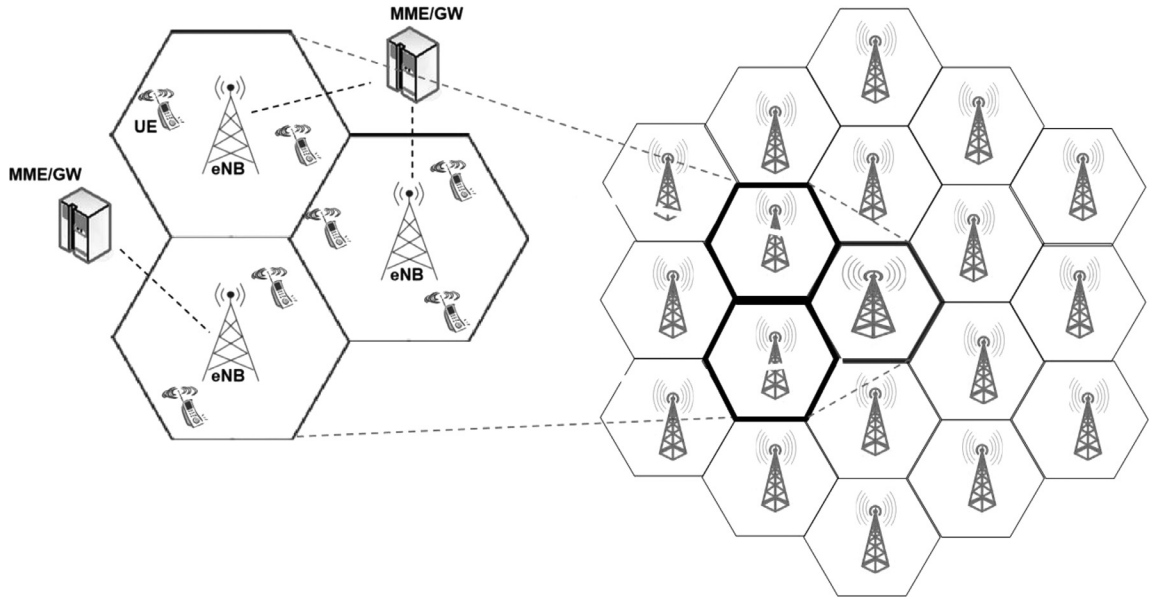

Fig. 5. The proposed network topology.

starts the first iteration by examining the best SINR threshold value in terms of the tradeoff between uplink signaling overhead and downlink performances; i.e. downlink throughput and outage capacity. This tradeoff is achieved by using SAW after initializing the priority weight per each objective function. Once the PSO finds the best threshold, a new population of the swarm is generated, and the second iteration starts to find the new best threshold value. This operation continues until the algorithm converges or the number of iterations is over. After that the SOPF algorithm will trigger the UE to tune the priority weight according to the PLR obtained after each transmission interval. If the obtained PLR is less than PLR_{tar}, the CQI overhead will be prioritized over the other criteria. On the contrary, if the obtained PLR is larger than PLR_{tar}, the priority weight corresponding to outage capacity will be maximized over the others. The serving eNodeB informs the UE about the resulted PLR at the current TTI via a 1-bit PLR status indicator (PSI) within the physical downlink control channel (PDCCH). When the resulted PLR is still below the acceptable threshold, the PSI is set to (0), and SOPF will increase the priority weight of uplink signaling overhead. Otherwise, the PSI is set to (1), and the SOPF will increase the priority weight of downlink parameters. Such flexible design will optimize the network performance by simply adjusting one parameter. According to the aforementioned procedure, the pseudo code of the SOPF algorithm is described in Table 2.

5. Complexity analysis

For the SOPF algorithm at the UE side, the main computational complexity of finding the optimal SINR threshold is related to the computations of PSO. In spite of its popularity, the PSO suffers from high computational complexity and high convergence time. Increasing the number of particles will decrease the convergence time, but it increases the computational complexity. Specifically, the number of operations required for a complete run of PSO algorithm is the sum of computations required to calculate the fitness function of a candidate solution and the computations required to update the position and velocity of each particle. Thus, three main things are required to be taken into account to minimize the computational complexity.

- Simplify the fitness function.
- Minimize the number of particles.
- Minimize the number of iterations.

Table 3
Simulation parameters.

Scenario	
No. of cells	19
Radius of cell (km)	1
Minimum no. of users per cell	3
Maximum no. of users per cell	30
Increased-step number of users	3
Number of simulations	20
Simulation time (s)	120
OFDM	
Carrier frequency (GHz)	2 GHz
Bandwidth (MHz)	10
No. of RBs	50
Mobility model	Random direction
Speed (km/h)	3
Channel model	
Environment	Macrocell with urban area
Shadowing	Long-normal distribution (mean= 0, standard deviation= 8 dB)
Penetration loss (dB)	10
Thermal noise (No) (dBm)	−174
Traffic-video	
Source	Video trace file
Encoder	H.264
Bit-rate (kbps)	242
Packet delay budget (ms)	150 (See Table 1)
Target packet loss ratio	0.1 (10%) [30]

In the SOPF algorithm, the computations of fitness function are already minimized such that only simple mathematical operations are included. From lines 5–16 of algorithm shown in Table 2, it is shown that the number of operations required to calculate the fitness function per each particle is $(3 \times N_{RB})$. On the other hand, minimizing both the number of particles and the number of iterations reduces the computational complexity but it may reduce the algorithm accuracy. Therefore, in SOPF, we first proposed to minimize the swarm size to not exceed 10 particles, and examined the algorithm under a different number of iterations. In the next section, it is shown that the results produced by using 20 iterations

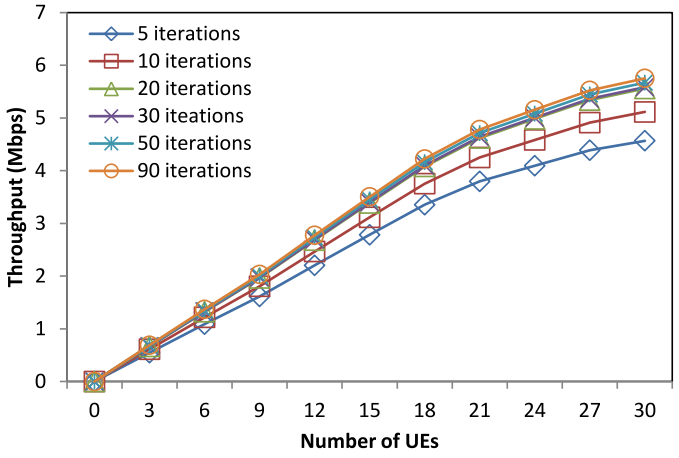

Fig. 6. Throughput vs number of iterations.

are slightly different from that produced by using a higher number of iterations. Therefore, the number of iterations is minimized to a value at which the difference in the obtained results is not significant. In terms of the complexity notation, the computational complexity of SOPF algorithm is $O(t)+O(1)=O(t)$, where t represents the number of iterations.

6. Simulation setup and performance evaluation

In this paper, a system-level simulation is performed by using the discrete event-driven LTE-Sim [30]. The simulated network topology is composed by a set of cells and network nodes (including eNodeBs, one or more Mobility Management Entity/Gateway MME/GW, and UEs), distributed among cells. The details of each node is explained in [30]. The considered scenario consists of 19 cells with up to 30 users moving along random paths within the central cell. The simulation is performed only in the central cell, while the other 18 cells are considered as generators of interference as shown in Fig. 5. Real-time guaranteed bit rate video flows are considered. A trace-based H.264 video file is used to generate the video flows [31]. The simulation parameters are listed in Table 3.

In this section, the performance of the proposed ATCPF algorithm is evaluated and compared with four of the state-of-the-art LTE feedback schemes, which are the full feedback, wideband feedback, subband-level feedback, and fixed threshold feedback. Moreover, different performance results are obtained when a different priority weight assignment is applied. First of all, the ATCPF with equal priority (ATEP) is evaluated and compared with the benchmarks. Then, the performance of the ATCPF is further evaluated when either feedback overhead (ATOhP), the outage (ATOP), or throughput (ATTP) is given the highest priority.

Since an iterative intelligent algorithm is used in our simulation, the number of iterations is an important parameter to be defined such that the computational complexity is minimized. Therefore, the system-level simulation is performed with different number of iterations to find out the minimum number of iterations required such that the system performances will be acceptable. From Fig. 6, it is shown that the worst throughput is achieved when the number of iterations is very low, e.g. 5 iterations. While the number of iterations is increasing, the system throughput is improved significantly. However, it is shown that a high number of iterations of more than 20 will not result in a significant improvement in system performance. On the other hand, Fig. 7 shows the of time required to execute the developed algorithm for different number of iterations. The algorithms are implemented by using the system level simulator (LTE-sim) on an Intel Core-i7 3.6 GHz based personal computer running Linux-Ubuntu operating system. In Fig. 7, the time required to simulate 100 of 10 ms LTE frames is computed. It is shown that the executional time is clearly increased when the proposed SOPF is implemented with the number of iterations of more than 20. Therefore, the number of iterations in our simulation is chosen to be 20 in order to not increase the computational and time complexity.

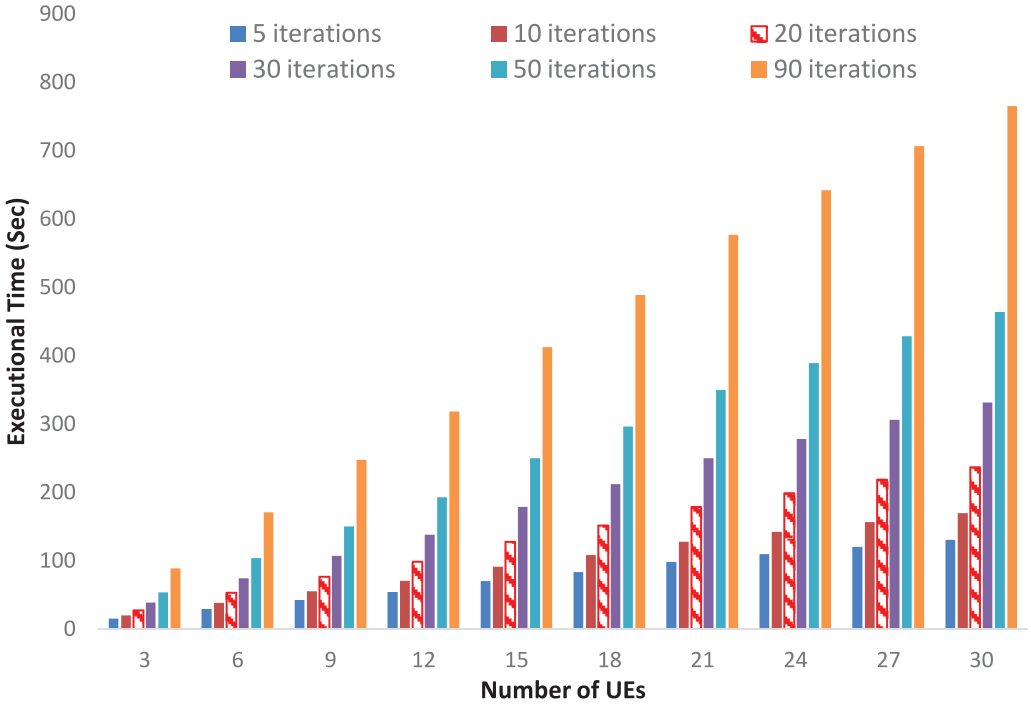

Fig. 7. Executional time vs nomber of UEs.

In a subband-level feedback, three different subband levels are examined, which are Subband-4 (Z = 4 subbands), Subband-6 (Z = 6 subbands), and subband-8 (Z = 8 subbands). Throughout this simulation, a significant overhead reduction of 84% can be obtained by using subband-4 compared to FFB as shown in Fig. 8(c). In this scheme, the entire channel bandwidth is divided into four subbands, each reports one CQI value which represents the averaged SINR of the entire RBs. Although, the throughput and packet loss ratio are improved compared to wideband feedback, the subband-level scheme is not an efficient solution for LTE cellular systems because of the relatively high loss in throughput compared to FFB, which is up to 63% when subband-4 is used as shown in Fig. 8(a). The downlink performances can be more improved when the number of selected subbands is increased. Particularly, when the channel bandwidth divided by eight subbands (subband-8), the PLR and throughput are enhanced as shown in Fig. 8(a and b) respectively. In other words, the more the number of channel subbands, the more robustness to fading of frequency selective channels, and the more gain in downlink performances at the cost of CQI overhead.

Unlike subband-level scheme which reports the averaged CQI values of RBs belonging to subband without considering their significance, the fixed threshold scheme proposes to report the averaged CQI value for the RBs belonging to the threshold window and reports another averaged value for remaining RBs. This scheme improves the throughput and PLR especially at a high number of users because of multi-user diversity gain. It is shown in Fig. 9(a) that the throughput achieved by a fixed 5 dB threshold based CQI scheme is closed to that obtained by subband-8 at low and intermediate traffic load. However, there is a 15% gain in throughput when the number of users increases to 30. Moreover, the PLR is reduced by 50% with a fixed 5 dB threshold compared to subband-8 as shown in Fig. 8(b) and 7(b). This remarkable improvement in downlink performances is obtained because the CQI words generated by the fixed-threshold based CQI scheme is more significant in reflecting the quality of the channel than that generated by subband-level scheme.

By using our proposed ATEP algorithm, a tradeoff between throughput, PLR and CQI overhead is considered. It is shown in Figs. 8 and 9 that the downlink performances are improved over that obtained by subband-level and fixed-threshold feedback schemes respectively with reasonable cost of feedback overhead. At high traffic load of 30 users, ATEP achieves the maximum gain in throughput of 40% compared to subband-8 (see Fig. 8(a)), and 20% compared to fixed 5 dB threshold feedback (see Fig. 9(a)). Moreover, the PLR is reduced by 69% compared to subband-8, and 38% compared to 5 dB threshold feedback scheme as shown in Figs. 8(b) and 9(b) respectively. For heavier-load network condition, the PLR still increases due to traffic conjestion and high inter-user and inter-cell interference. Although the subband-level and fixed-threshold feedback schemes outperformed ATEP in terms of CQI overhead, it is shown in Fig. 8(c) that the overhead is reduced by 41% compared to FFB, which is considered reasonable for such applications. By using our analytical model and the iterated PSO, the obtained optimal threshold window of CQI feedback leads to improve the objective function which aims to find the tradeoff between throughput, outage capacity and overhead. We further modified our analytical approach to provide unequal fixed priorities for the conflicting objectives according to network or user preferences. Fig. 10 compares the performance between the approach with equal and unequal priorities. It is shown that the throughput (Fig. 10(a)) and PLR (Fig. 10(b)) are maximized when the outage capacity is given a maximum priority (ATOP), but at the cost of signaling overhead (Fig. 10(c)) which performs the worst among the others. In other words, ATOP searches for the threshold value at which the outage is minimized and, thus, the PLR and

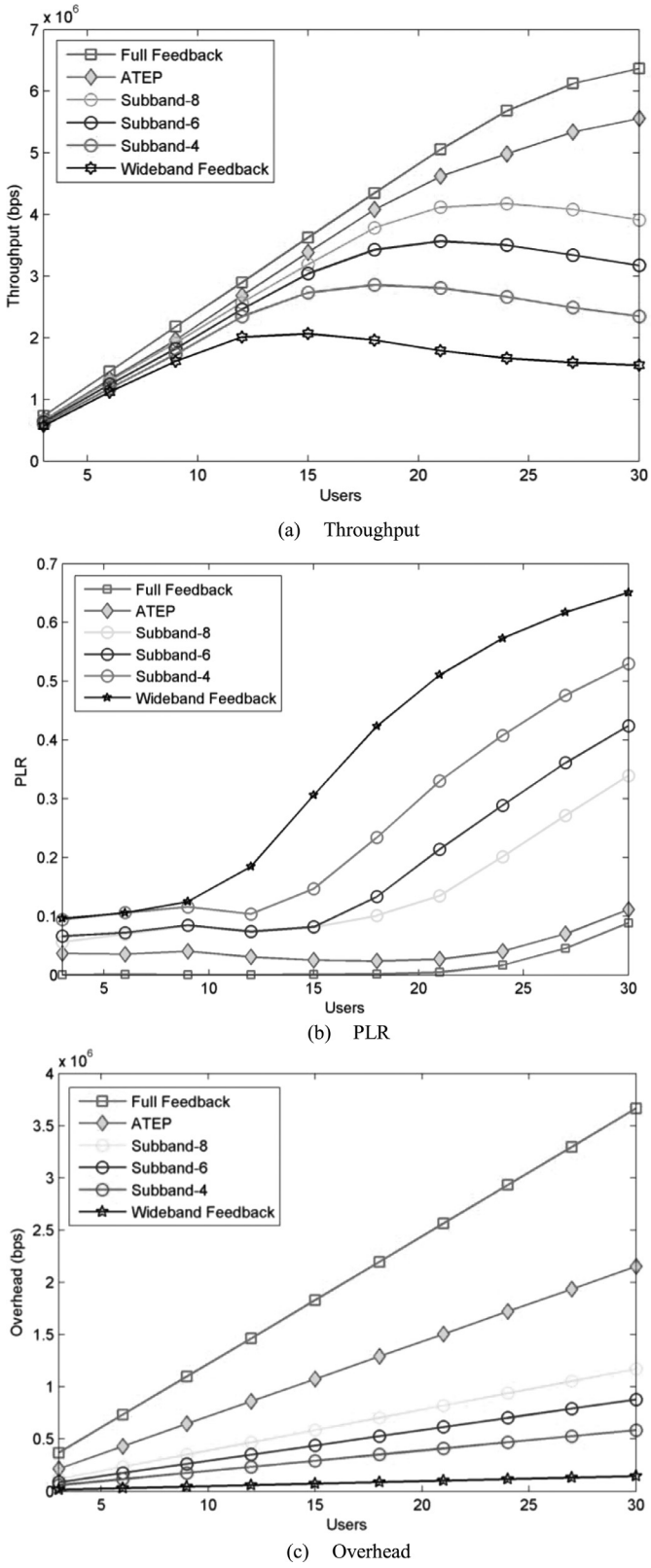

Fig. 8. Performance comparison between the proposed ATEP and subband-level algorithm.

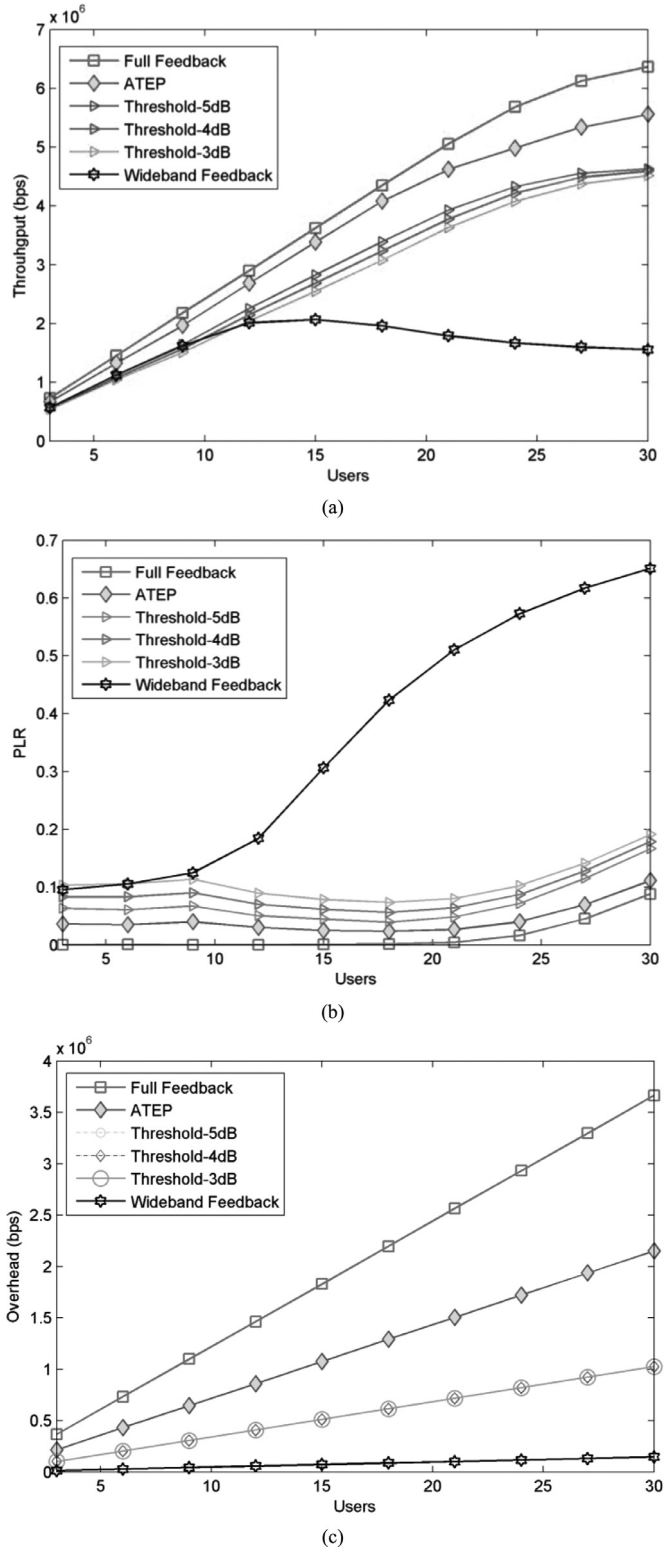

Fig. 9. Performance comparison between proposed ATEP and fixed threshold based feedback scheme.

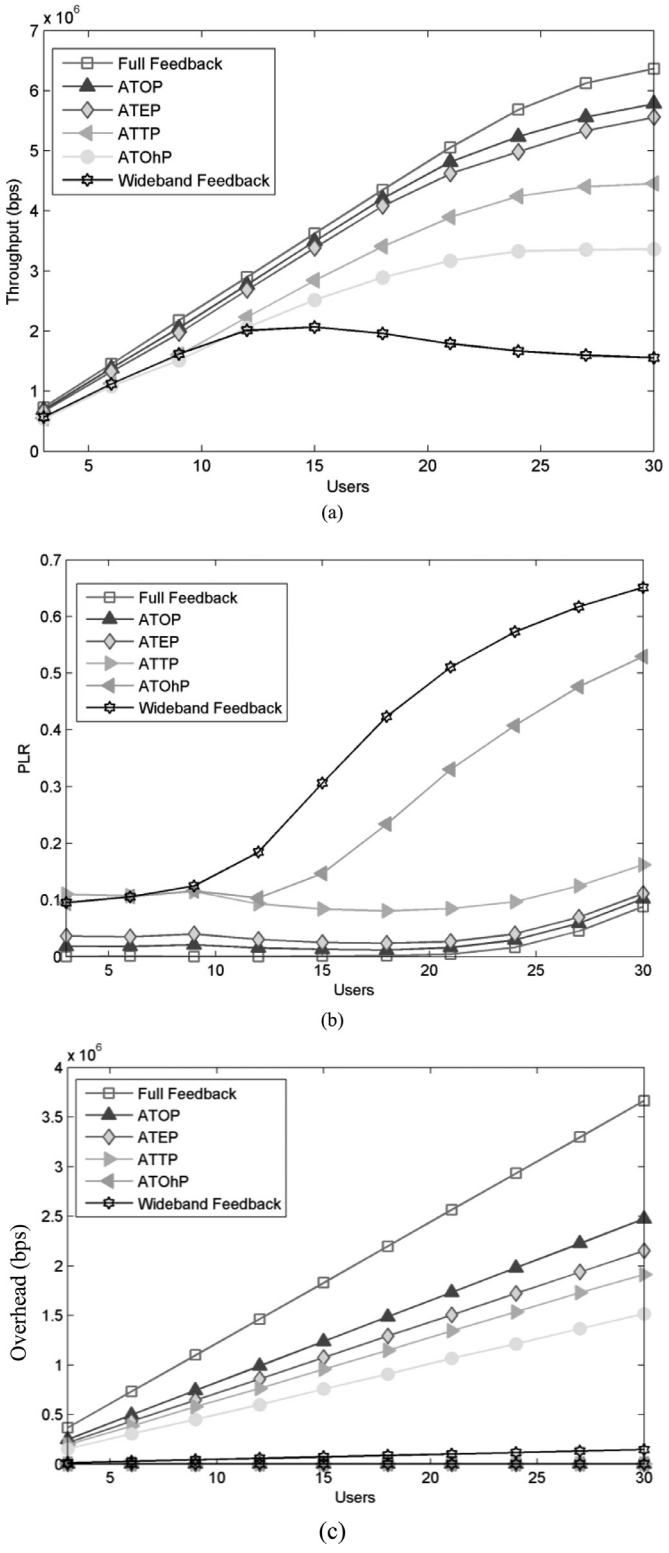

Fig. 10. Performance comparison between equal and unequal weight priorities for the proposed algorithm.

throughput will be maximized. However, the CQI signaling overhead is reduced to the lowest possible when it is given maximum priority (ATOhP) at the cost of throughput and PLR as shown in Fig. 10(a,b, and c).

In order to find the best solution in terms of overall system metrics, a weighted product model (WPM) [32] is used to compare between our scheme and the other aforementioned schemes. Since the throughput represents a benefit criterion while the PLR and overhead represents cost criteria, the overall feedback optimization product (FOP) can be represented as

$$FOP_k = \sum_{k=0}^{K} \frac{R_k}{\phi_k \times PLR_k}, \quad \forall k \in K \tag{24}$$

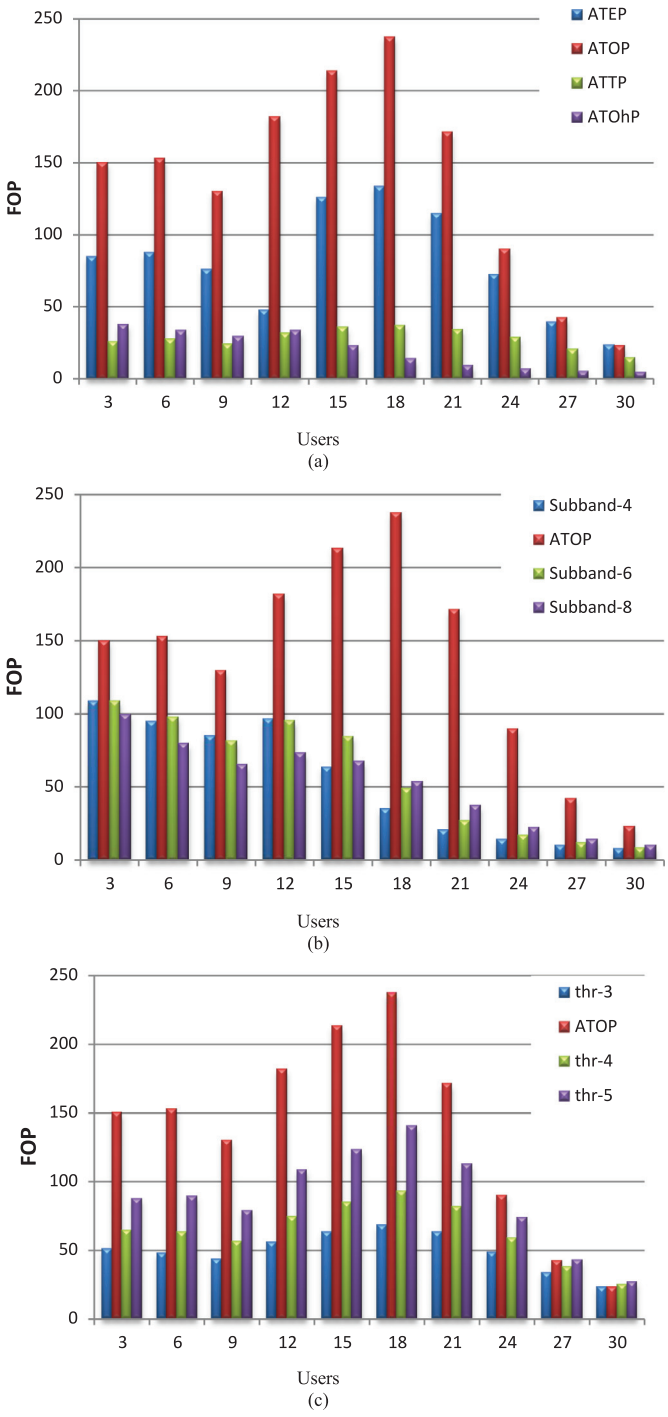

Fig. 11. A comparison of FOP between the proposed algorithms.

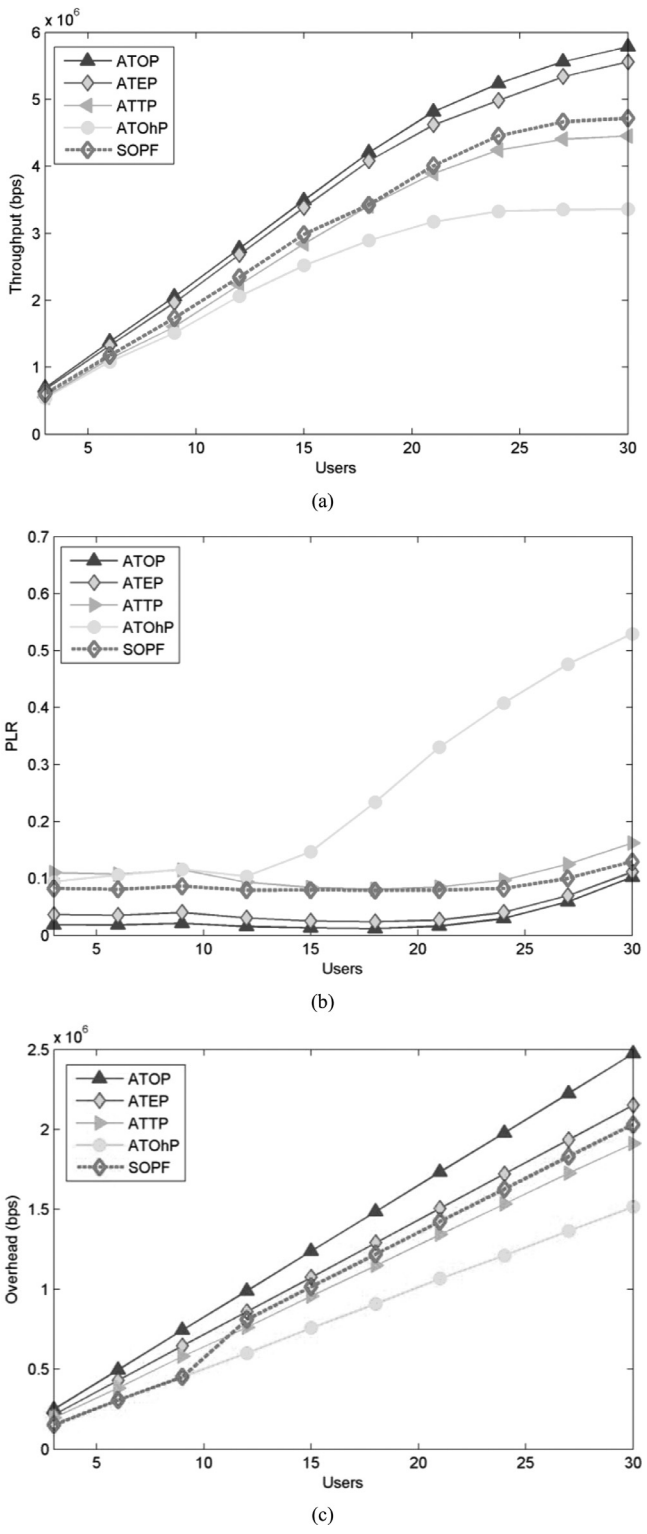

Fig. 12. Performance comparison between fixed and adaptive weight priorities for the proposed algorithm.

It is shown in Fig. 11(a) that the ATOP scheme can give the best FOP compared to ATEP, ATTP, and ATOhP. Furthermore, ATOP gives the best FOP compared to both subband-level scheme (see Fig. 11(b)) and fixed threshold based scheme (see Fig. 11(c)). In other words, the ATOP scheme can achieve the best tradeoff between CQI signaling overhead and LTE downlink performance.

For the SOPF Algorithm, we modified ATEP algorithm to have an adaptive priority weight assignment by using cross-layer optimization. This optimization aims to guarantee QoS of different real-time multimedia services by adapting the priority weight according to targeted PLR. Fig. 12 compares between the performance of the proposed approach when the fixed and adaptive weight assignments are used. It is shown that the signaling overhead can be minimized as long as the PLR below its target. Once the number of users increases to more than 15, the PLR starts to increase to more than its threshold due to high traffic load and, thus, the weight priority is given to outage and throughput rather than the overhead. Particularly, more signaling overhead is required when the num-

ber of users increases to enable frequency scheduling. Otherwise, wrong scheduling decisions will be made by eNodeB which lead to increasing the number of dropped packets due to wrong decoding process.

7. Summary and conclusion

Reducing the amount of CQI signaling overhead is crucial for saving energy and bandwidth of a UE. However, the reduction in channel feedback information results in downlink performance degradation, and might sacrifice the QoS when real time multimedia services are targeted. In this paper, the relationship between CQI overhead and LTE downlink performances was analyzed. It is revealed that the more signaling overhead to report the channel quality at the uplink, the more throughput can be achieved at the downlink transmission with less outage capacity. Accordingly, the ATCPF algorithm is developed to find the best tradeoff between uplink and downlink performances by using a hybrid of swarm intelligence and SAW. Based on the system level simulation, the ATCPF algorithm has achieved the best FOP compared with the fixed-threshold and subband level feedback schemes, especially when the maximum priority is assigned to the outage capacity (ATOP). Moreover, the SOPF algorithm is proposed to guarantee QoS for video traffic. It is shown that the signaling overhead can be minimized to the lowest possible as long as the video flows are correctly received by UEs. The developed scheme provides a high flexibility in responding to various network conditions without applying complicated modifications. Generalizing the proposed algorithm for real-time applications other than video streaming is possible as long as the QoS parameter is specified. For non-real time traffic, the QoS constraint will be relaxed for the benefit of other system performances. In addition to CQI feedback, the precoding matrix and rank indicators are also required to be incorporated in the future work when MIMO-based LTE systems are investigated.

Appendix A

The EESM mapping is derived from the Chernoff union bound for bit error rates [33]. The probability of error *Pe* for Binary Phase Shift Keying (BPSK) transmission over an AWGN channel is given by

$$P_e(\gamma_z, d) = Q\left(\sqrt{2}\gamma_z\right) \tag{A.1}$$

where d is represented the symbol distance and assumed to be 1 and γ_z is indicated the SINR$_z$. In order to find the upper bounded SINR$_z$, the Chernoff union bound will be carried out according to

$$P_e(\gamma_z, 1) \le e^{-\gamma_z} \tag{A.2}$$

For the purpose of transmissions over N AWGN channels, the probability of given at least one error will be as

$$P_e = 1 - \prod_{z=1}^{Z} (1 - P_e(\gamma_z)) \approx \sum_{z=1}^{Z} e^{-\gamma_z} \tag{A.3}$$

The result is the error rate for a block of Z REs, each of which consists of different symbols. Therefore, the target is to achieve an SNR_{eff} value γ_{eff} equivalent to P_e. Thus, in (A.5) $\gamma_z = \gamma_{eff}$ so that

$$\mathrm{Re}^{-\gamma_{eff}} = \sum_{z=1}^{Z} e^{-\gamma_z} \tag{A.4}$$

By solving the γ_{eff}, Eq. (A.1) is rewritten as

$$\gamma_{eff} = -\ln \frac{1}{Z} \sum_{z=1}^{Z} e^{-\gamma_z} \tag{A.5}$$

In order to find the Quadrature Phase Shift Keying (QPSK) the same derivation can be made. QPSK is represented by 2 bits, then the exponential ESM becomes as

$$\mathrm{SINR}_{\mathrm{eff}} = \gamma_r = -\lambda \ln \frac{1}{Z} \sum_{z=1}^{Z} e^{-\frac{\gamma_z}{\lambda}} \tag{A.6}$$

where λ is a parameter that is empirically calibrated for each MCS.

References

[1] R. Knopp, P.A. Humblet, Information capacity and power control in single-cell multiuser communications, Communications, 1995. ICC'95 Seattle,'Gateway to Globalization', 1995 IEEE International Conference on, IEEE, 1995.

[2] C.Y. Wong, et al., Multiuser OFDM with adaptive subcarrier, bit, and power allocation, Selected Areas Commun. IEEE J. 17 (10) (1999) 1747–1758.

[3] M. Ergen, S. Coleri, P. Varaiya, QoS aware adaptive resource allocation techniques for fair scheduling in OFDMA based broadband wireless access systems, Broadcast. IEEE Trans. 49 (4) (2003) 362–370.

[4] 3GPP, 3GPP TS 36.213 V10.5.0- Technical specification group radio access network; evolved universal terrestrial radio access (E-UTRA); Physical layer procedures, *2012*: Valbonne – France.

[5] S.V. Tran, A.M. Eltawil, Link adaptation for wireless systems, Wireless Commun. Mob. Comput. 14 (16) (2014) 1509–1521.

[6] M.I. Salman, et al., A self-configured link adaptation for green LTE downlink transmission, Trans. Emerg. Telecommun. Technol. (2014).

[7] F. Florén, O. Edfors, B.-A. Molin, The effect of feedback quantization on the throughput of a multiuser diversity scheme, Global Telecommunications Conference, 2003. GLOBECOM'03. IEEE, IEEE, 2003.

[8] Y.-J. Choi, S. Bahk, Selective channel feedback mechanisms for wireless multichannel scheduling, in: Proceedings of the 2006 International Symposium on on World of Wireless, Mobile and Multimedia Networks, IEEE Computer Society, 2006.

[9] P. Svedman, et al., Opportunistic beamforming and scheduling for OFDMA systems, Commun. IEEE Trans. 55 (5) (2007) 941–952.

[10] S. Guharoy, N. Mehta, Joint evaluation of channel feedback schemes, rate adaptation, and scheduling in OFDMA downlinks with feedback delays, IEEE T. Vehic. Technol. 62 (4) (2013) 1719–1731 2013.

[11] T. Tang, R.W. Heath, Opportunistic feedback for downlink multiuser diversity, IEEE Commun. Lett. 9 (10) (2005) 948–950.

[12] M.Q. Abdulhasan, et al., An adaptive threshold feedback compression scheme based on channel quality indicator (CQI) in long term evolution (LTE) system, Wireless Person. Commun. (2015) 1–27.

[13] N. Kolehmainen, et al., Channel quality indication reporting schemes for UTRAN long term evolution downlink, Vehicular Technology Conference, 2008. VTC Spring 2008. IEEE, IEEE, 2008.

[14] Y.-J. Choi, S. Bahk, Partial channel feedback schemes maximizing overall efficiency in wireless networks, Wireless Commun. IEEE Trans. 7 (4) (2008) 1306–1314.

[15] C. Diao, M. Chen, B. Wu, Comments on" Partial channel feedback schemes maximizing overall efficiency in wireless networks, Wireless Commun. IEEE Trans. 10 (3) (2011) 1006–1008.

[16] J. Chen, R.A. Berry, M.L. Honig, Limited feedback schemes for downlink OFDMA based on sub-channel groups, Selected Areas Commun. IEEE J. 26 (8) (2008) 1451–1461.

[17] S.N. Donthi, N.B. Mehta, An accurate model for EESM and its application to analysis of CQI feedback schemes and scheduling in LTE, Wireless Commun. IEEE Trans. 10 (10) (2011) 3436–3448.

[18] S.N. Donthi, N.B. Mehta, Joint performance analysis of channel quality indicator feedback schemes and frequency-domain scheduling for LTE, Vehic. Technol. IEEE Trans. 60 (7) (2011) 3096–3109.

[19] M. Torabi, D. Haccoun, W. Ajib, Performance analysis of scheduling schemes for rate-adaptive MIMO OSFBC-OFDM systems, Vehic. Technol. IEEE Trans. 59 (5) (2010) 2363–2379.

[20] A. Kuhne, A. Klein, Throughput analysis of multi-user OFDMA-systems using imperfect CQI feedback and diversity techniques, Selected Areas Commun. IEEE J. 26 (8) (2008) 1440–1450.

[21] Y. Du, et al., Evaluation of PMI feedback schemes for MU-MIMO pairing, Syst. J. IEEE 4 (4) (2010) 505–510.

[22] M. Kang, et al., Partial feedback schemes for MIMO–OFDMA systems using random beamforming: analysis and optimization, Wireless Commun. Mob. Comput. 14 (6) (2014) 596–612.

[23] M.Q. Abdulhasan, et al., Review of channel quality indicator estimation schemes for multi-user MIMO in 3GPP LTE/LTE-a systems, KSII Trans. Internet Inf. Syst. (TIIS) 8 (6) (2014) 1848–1868.

[24] S. Ko, et al., Mode selection-based channel feedback reduction schemes for opportunistic scheduling in OFDMA systems, Wireless Commun. IEEE Trans. 9 (9) (2010) 2842–2852.

[25] M. Pauli, S.-H.S. Tsai, U. Wachsmann, Quality determination for a wireless communications link, Google Patents (2007).

[26] J. Kennedy, J.F. Kennedy, R.C. Eberhart, Swarm Intelligence, Morgan Kaufmann, 2001.

[27] K.P. Yoon, C.-L. Hwang, Multiple Attribute Decision Making: an Introduction. Vol. *104*, Sage Publications, 1995.

[28] Y. Del Valle, et al., Particle swarm optimization: basic concepts, variants and applications in power systems, Evol. Comput. IEEE Trans. 12 (2) (2008) 171–195.
[29] Y. Shi, R. Eberhart, et al., Parameter selection in particle swarm optimization, in: V.W. Porto, et al. (Eds.), Evolutionary Programming VII, Springer, Berlin Heidelberg, 1998, pp. 591–600.
[30] G. Piro, et al., Simulating LTE cellular systems: an open-source framework, Vehic. Technol. IEEE Trans. 60 (2) (2011) 498–513.
[31] Video trace library," [OnLine] Available. Available from: http://trace.eas.asu.edu/.
[32] E. Triantaphyllou, Multi-Criteria Decision Making Methods a Comparative Study, Springer, 2000.
[33] R. Sandanalakshmi, T. Palanivelu, K. Manivannan, Effective SNR mapping for link error prediction in OFDM based systems, in: Information and Communication Technology in Electrical Sciences (ICTES 2007), 2007. ICTES. IET-UK International Conference on, 2007, pp. 684–687.

Mustafa Ismael Salman received the B.*Sc*. degree in electronic and communications engineering from Al-Nahrain University, Iraq, 2000. Then, he received the M.*Sc*. in modern communications from Al-Nahrain University, Iraq, 2003. Since 2003, he is working as a senior lecturer in University of Baghdad, teaching many subjects in the field of computer and communications engineering. Then, he received PhD in Wireless Communications Engineering at Universiti Putra Malaysia. Currently, He is a senior lecturer in University of Baghdad. His main research interests are green cellular networks, 3GPP LTE networks, OFDM networks, and adaptive resource allocation in cellular networks.

Muntadher Qasim Abdulhassan received the B.*Sc*. degree in Electrical Engineering from Baghdad University, Iraq, in 2007. He is currently an M.*Sc* student in Wireless Communication Engineering at Universiti Putra Malaysia. His main research interests are in wireless communication system design with main emphasis on multiple – input multiple output (MIMO) system and orthogonal frequency division multiplexing (OFDM), and power efficiency.

Chee Kyun Ng received his Bachelor of Engineering and Master of Science degrees majoring in Computer & Communication Systems from Universiti Putra Malaysia, Serdang, Selangor, Malaysia, in 1999 and 2002 respectively. He has also completed his PhD programme in 2007 majoring in Communications and Network Engineering at the same university. He is currently undertaking his research on wireless multiple access schemes, wireless sensor networks and smart antenna system. His research interests include mobile cellular and satellite communications, digital signal processing, and network security. Along the period of his study programmes, he has published over 100 papers in journals and in conferences.

Nor Kamariah Noordin received her BSc in Electrical Engineering majoring in Telecommunications from University of Alabama, USA, in 1987. She became a tutor at the Department of Computer and Electronics Engineering, Universiti Putra Malaysia, and pursued her Masters Degree at Universiti Teknologi Malaysia and PhD at Universiti Putra Malaysia. She then became a lecturer in 1991 at the same department where she was later appointed as the Head from year 2000 to 2002. She is currently the Deputy Dean (Academic, Student Affairs and Alumni) of the Faculty. During her more than 15 years at the department she has been actively involved in teaching, research and administrative activities. She has supervised a number of undergraduate students as well as postgraduate students in the area of wireless communications, which led to receiving some national and UPM research awards. Her research work also led her to publish more than 100 papers in journals and in conferences.

Borhanuddin bin Mohd Ali obtained his BSc (Hons) Electrical and Electronics Engineering from Loughborough University in 1979; MSc and PhD from University of Wales, UK, in 1981 and 1985, respectively. He became a lecturer at the Faculty of Engineering UPM in 1985, made a Professor in 2002, and Director of Institute of Multimedia and Software, 2001–2006. In 1997 he co founded the national networking testbed project code named Teman, and became Chairman of the MYREN Research Community in 2002, the successor to Teman. His research interest is in Wireless Communications and Networks where he publishes over 80 journal and 200 conference papers. He is a Senior Member of IEEE and a member of IET and a Chartered Engineer, and the present ComSoc Chapter Chair. He is presently on a 2-year secondment term with Mimos as a Principal Researcher, heading the Wireless Networks and Protocol Research Lab.

Aduwati Sali is currently a Lecturer at Department of Computer and Communication Systems, Faculty of Engineering, Universiti Putra Malaysia (UPM) since July 2003. She obtained her PhD in Mobile Satellite Communications form University of Surrey, UK, in July 2009, her MSc in Communications and Network Engineering from UPM in April 2002 and her BEng in Electrical Electronics Engineering (Communications) from University of Edinburgh in 1999. She worked as an Assistant Manager with Telekom Malaysia Bhd from 1999 until 2000. She involved with EU-IST Satellite Network of Excellence (SatNEx) I & II from 2004 until 2009. She is the principle investigator for projects under the funding bodies Malaysian Ministry of Science, Technology and Innovation (MOSTI), Research University Grant Scheme (RUGS) UPM and The Academy of Sciences for the Developing World (TWAS-COMSTECH) Joint Grants. Her research interests are radio resource management, MAC layer protocols, satellite communications, wireless sensor networks, disaster management applications, 3D video transmissions.